

Cyclic Motion of a Grafted Polymer under Shear Flow

Rafael Delgado-Buscalioni*

*Departamento de Ciencias y Técnicas Fisicoquímicas, Universidad de Educación a Distancia,
C/Senda del Rey, 9, Madrid 28040, Spain*

(Received 21 October 2005; published 2 March 2006)

The long-time dynamics of a single end-tethered chain under shear flow are studied using molecular and Brownian dynamics simulations of a flexible polymer. As observed in previous experiments with tethered DNA [Phys. Rev. Lett. **84**, 4769 (2000)], under a flow sheared at constant rate $\dot{\gamma}$ the chain performs a cyclic motion. But, contrary to what has been previously suggested, a well-defined characteristic period exists and it is clearly revealed in the cross spectra of the chain extension along flow and gradient directions. The main cycling time scales like the time needed to stretch the polymer by convection, being about 10 times the relaxation time of the chain in flow. This coherent recursive motion introduces long memory in the fluid and suggests resonance effects under periodic external forcing.

DOI: 10.1103/PhysRevLett.96.088303

PACS numbers: 36.20.-r, 83.10.Rs, 83.50.Ax

The ability to visualize individual polymers via fluorescent staining [1] has revealed that many nontrivial macroscopic properties of polymeric fluids cannot be inferred from ensemble averages alone, but rather from the individual chain dynamics [2]. Strikingly, the behavior of individual chains in nonequilibrium can greatly differ from one to another, providing extremely rich dynamics when exposed to shear [3] or elongational flow [1]. One related fact is that the chain-flow interaction can be articulated over long characteristic times, much longer than the natural relaxation time of the chain. These long characteristic times are directly related to many properties of polymeric systems such as fluid memory or the strong resonance observed in polymer brushes [4], single tethers [5], or proteins [6], under periodic external perturbations.

Tether polymers provide an excellent illustration of the above ideas. For instance, tethers are relevant in several biological processes, such as the ligand-receptor binding [5,7] whereby the chains need to extend well beyond their equilibrium conformation to promote the adhesion of adjacent cells. Interestingly, the efficiency of this process depends more on the long-time dynamics of the tethering chain via the occurrence of “rare” extended conformations, rather than on its equilibrium conformation [7]. As shown in recent simulations, flow disturbances may also have a significant effect as the radius of gyration of the tether can dramatically increase if an external oscillatory force with a low enough frequency is imposed in the normal-to-wall direction [5].

The dynamics of tether chains under flow are relevant for many other technological applications, such as stabilization of colloidal suspensions, lubrication, chromatography, adhesion [2], or drag reduction. Albeit most previous experiments and numerical simulations focused on the effect of flow on static properties [8–10], a more recent experimental study on the dynamics of individual DNA chains under steady shear, by Doyle *et al.* [2], demonstrated that the chain performs cyclic dynamics arising

from a complex chain-flow interaction. These authors suggested that the cyclic dynamics are aperiodic, as the power spectrum of the chain extension along flow direction does not exhibit distinct peaks. This Letter reconsiders this issue by analyzing the cross correlation of chain extension in orthogonal directions. An important question is to determine whether the chain-flow interaction is completely aperiodic or articulated within well-defined characteristic times. Contrary to previous suggestions, this work presents a clear indication that the long-time dynamics of the tether has a preferential cycling time. These low frequencies could be the origin of resonant effects, which are known to occur in many different contexts such as those reported for brushes in oscillatory shear flow [4].

Methods.—The system considered is depicted in Fig. 1(a). A fluid fills the space between two walls and, due to the motion of the upper wall, is subject to a constant shear. A single polymer is tethered to the bottom wall and explicitly interacts with solvent particles (Lennard-Jones fluid) and wall atoms [11]. The present setup contrasts with previous published simulations [8–10], which considered purely reflecting walls and no explicit solvent. The polymer is modeled using the bead-spring model of Kremer and Grest [12]: the nonextensible chain is formed by $N = 60$ monomers linked by the finite extensible nonlinear elastic potential $U_{nn}(r_{ij}) = -\frac{1}{2}kR_0^2 \ln[1 - (r_{ij}/R_0)^2]$ (where r_{ij}

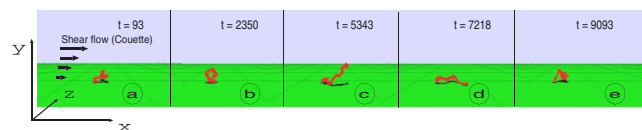


FIG. 1 (color online). Tethered polymer under shear flow from a MD simulation with $Wi = 2$. Each figure shows 25 successive superimposed snapshots of the chain, covering a time interval of $[t, t + 9.375]$. The sequence (a)–(e) illustrates the “cyclic dynamics” observed at time scales longer than its relaxation time, which for this case is 1250τ . Time is given in LJ units (τ).

is the distance between neighboring beads, $R_0 = 1.5\sigma$, $k = 30\epsilon/\sigma^2$). The mass, length, energy, and time scales are set by the standard Lennard-Jones (LJ) units: m (monomer mass), σ , ϵ , and $\tau = \sigma\sqrt{m/\epsilon}$, respectively. Further details on the molecular dynamics (MD) model are given in Barsky *et al.* [13]. Simulations were carried out using standard MD in a slit of dimensions $(38 \times 50 \times 33)\sigma$ and using the hybrid particle-continuum model developed by Delgado-Buscalioni *et al.* [14]. The hybrid method reduces the MD domain to a small volume around the chain while the solvent flow outside is solved using continuum fluid dynamics (see [13,14] for details). As in previous works [13] on the polymer structure, the hybrid model is found to be in perfect agreement with standard MD results, so in the foregoing discussion they will be both referred to as “MD.” As a qualitatively different model, we also performed Brownian dynamics (BD) simulations of free draining chains interacting with the same potential used in the MD simulations. The bead diffusion constant was set to 0.42. Analysis of the long-time dynamics required quite long trajectories: more than 1000 times the BD chain relaxation time under shear flow and more than 500 in the case of the MD chain.

Relaxation times.—The dynamics of a single polymer under flow is determined by the Weissenberg number, $Wi \equiv \dot{\gamma}\tau_0(0)$, which gives the ratio of $\tau_0(0)$, the polymer relaxation time at equilibrium ($\dot{\gamma} = 0$), and the flow characteristic time $1/\dot{\gamma}$. The longest relaxation time of the chain is given by the decorrelation time of the lowest normal mode. In the linear approximation to the chain dynamics, the normal coordinates [15] for a tether are [16] $\hat{\mathbf{R}}_p(t) = (1/N)\sum_{n=0}^N \mathbf{R}_n(t) \sin[(p + 1/2)\pi n/N]$, where \mathbf{R}_n denotes the positions of the chain beads. The longest polymer relaxation time was estimated from simulations by fitting the autocorrelation of $\hat{X}_0 \equiv \hat{\mathbf{R}}_0 \cdot \mathbf{i}$ to a single exponential function (similar relaxation times, within error bars, were obtained from the decorrelation time of the end-to-end vector.) The resulting values under no flow condition were used to calculate the Weissenberg number for each model. For chains with $N = 60$ beads, we obtained $\tau_0(0) = (4000 \pm 200)\tau$ and $(2000 \pm 500)\tau$ in BD and MD simulations, respectively. Consistently with the free draining limit [16], in BD simulations, the relaxation times of the faster modes ($p > 0$) were observed to decay like $\tau_p(0) \sim (p + 1/2)^{-2.1 \pm 0.1}$. By contrast, MD simulations give $\tau_p(0) \sim (p + 1/2)^{-1.6 \pm 0.1}$, indicating the presence of hydrodynamic interactions induced by the explicit solvent. However, as shall be shown below, the main features of the chain dynamics occurring at longer time scales, are not related to solvent induced hydrodynamic interactions.

At $Wi > 1$ the flow starts to stretch the polymer average configuration [2,9,13], because the fluid elements deform faster than the polymer can possibly relax. As it will soon come clear, the dependence of the longest relaxation time

on the Weissenberg number, $\tau_0 = \tau_0(Wi)$ is also important to understand the chain dynamics at longer time scales. For $Wi > 2$, the best fits to the simulation results are $\tau_0(Wi) \approx 1.6\tau_0(0)Wi^{-0.70}$ and $\tau_0(Wi) \approx 0.9\tau_0(0)Wi^{-0.78}$ in the case of MD and BD simulations, respectively. These slopes are in agreement with the following scaling argument. Assuming that the chain deforms affinely with the fluid element, the average time required by the shear flow to stretch the chain a fraction α of its contour length L is given by $t_s \approx \alpha L / (\langle Y \rangle \dot{\gamma})$, with $\langle Y \rangle$ being the average extension of the polymer in the gradient direction ($Y \equiv \max\{Y_i\} - \min\{Y_i\}$, where Y_i is the y coordinate of the i th monomer in the chain). From MD and BD simulations $\langle Y \rangle \sim \dot{\gamma}^{-0.32}$ and $\langle Y \rangle \sim \dot{\gamma}^{-0.23}$, respectively. These slopes are consistent [17] with the theoretical scalings for $\langle Y \rangle$ proposed in the literature [9,18–20] and provide $t_s \sim Wi^{-0.68}$ and $t_s \sim Wi^{0.77}$, in good agreement with the trends obtained for the relaxation time for MD and BD simulations, respectively. This simple scaling indicates that in steady shear flow the relaxation time of a tethered chain scales nearly like the convective time required by the flow drag to stretch it. As an aside, experiments on conformational dynamics of individual free flexible polymers in steady shear flow [3] also reported a slope close to $-2/3$ for the relation between the chain relaxation time and Wi .

Cyclic dynamics.—At time scales much larger than its longest relaxation time the anchored polymer describes a continuous recirculating motion which, after the experiments with tethered DNA by Doyle *et al.* [2], is known as *cyclic dynamics*. Figure 1 illustrates one cycle of a chain at $Wi = 2$ obtained from MD simulations, covering a time interval of about 9000τ [note that for $Wi = 2$ the chain relaxation time is $\tau_0 = (1250 \pm 100)\tau$]. In Fig. 1(a) the polymer starts in a coiled configuration and eventually experiences a thermal fluctuation along y direction. This leads to a slightly extended configuration, like that in Fig. 1(b). The flow drag increases linearly with the y coordinate and therefore any expansion in the gradient direction induces a rapid elongation along the flow direction [Fig. 1(c)]. While being extended, the flow drag and

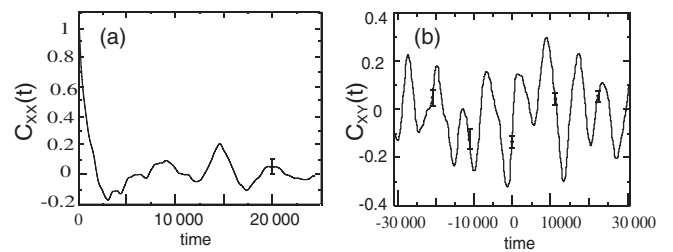


FIG. 2. (a) The normalized autocorrelation of the chain extension along flow direction X . (b) The cross correlation between X and the chain extension in gradient direction Y . Results are obtained from MD simulations of one chain at $Wi = 2$ and during a sampling time of $10^5\tau$; error bars come from the standard deviation of $\delta X(t)\delta Y(0)$.

the constraint to the wall creates a pair of forces which induce the subsequent rotation of the polymer towards the surface [Fig. 1(d)]. There, the flow drag vanishes and the polymer coils back to the configuration of Fig. 1(e). It is noticed that this recursive coil-stretching transition does not produce any periodic behavior in the time series associated with the polymer extension along any direction (not shown). Also, Doyle *et al.* [2] pointed out that the power spectra of the time series obtained from the polymer extension along flow direction do not present any distinct peaks. In fact, as shown in Fig. 2(a), the long-time behavior of the autocorrelation of the maximum chain extension in flow direction $X = \max\{X_i\} - \min\{X_i\}$ does not clearly indicate a characteristic recursion time. However, such quantity is not the best suited to characterize the mechanism involved in the cycling dynamics. As explained, the polymer successively “flaps” in the flow-gradient plane (xy), so a more natural measure for the analysis of the cycling motion is the cross correlation between the chain extension along flow and gradient directions, calculated as

$$C_{XY}(t) \equiv \frac{\langle \delta X(t) \delta Y(0) \rangle}{\sqrt{\langle \delta X(0)^2 \rangle \langle \delta Y(0)^2 \rangle}}. \quad (1)$$

Here $\delta X(t) = X(t) - \langle X \rangle$ and $\langle \cdot \rangle$ denotes time average. Figure 2(b) shows that the cross correlation between chain extension in flow and gradient directions reveals surprisingly well the presence of a characteristic period. Let us call T_{cycle} the main period of the cross correlation C_{XY} . During the first part of the cycle, $C_{XY}(t) > 0$, so a chain stretched in the gradient direction [$\delta Y(0) > 0$] will, most probably, become stretched [$\delta X(t) > 0$] at lagging times $0 < t < T_{\text{cycle}}/2$. During the second half of the cycle, $C_{XY}(t) < 0$, indicating that the polymer coils back [$\delta X(t) < 0$]. This oscillation of $C_{XY}(t)$ is also consistent with a chain that starts close to the surface [$\delta Y(0) < 0$], retracts to a coiled state [$\delta X(t) < 0$] over $t < T_{\text{cycle}}/2$ and stretches during $t > T_{\text{cycle}}/2$. In conclusion, $C_{XY}(t)$ indicates a clockwise chain recirculation in the xy plane. As an aside, we observed that the polymer motion produces a smaller but significant cross correlation in the (xz) flow-vorticity plane (not shown). Many experiments using fluorescence videomicroscopy can only observe a projection of the instantaneous polymer configurations in this plane, so this fact could facilitate the experimental confirmation of the present findings.

In order to investigate large scale structural correlations of the chain we calculated the cross power spectral density (CPSD) [21] associated with the chain extension in flow and gradient direction. As shown in Fig. 3 a peak is clearly observed in CPSD obtained from MD and BD simulations. It is noted that frequencies in Fig. 3 have been scaled with the chain relaxation time in flow $\tau_0(\dot{\gamma})$. As in previous works [18], at moderate and large frequencies $\omega\tau_0(0) > 1$ the slope of the power spectra depends on Wi and on the

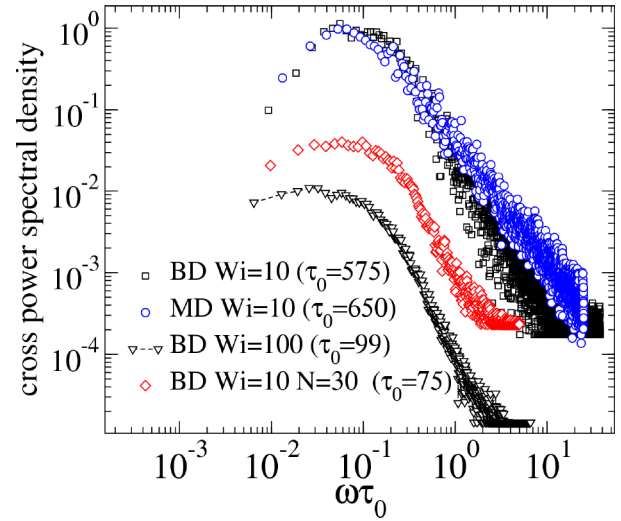


FIG. 3 (color online). CPSD of the chain extension in flow and gradient directions, X and Y . Frequencies are scaled with the relaxation time in flow $\tau_0(Wi)$ (values indicated in the figure) and the CPSD are normalized with the maximum value (some curves has been displaced for clarity). Diamonds corresponds to a chain with $N = 30$ beads, while the rest to $N = 60$.

presence of hydrodynamic interactions. However, upon scaling, the peak frequency obtained for different Wi and draining regimes merges to a similar value, $\omega_{\text{peak}}\tau_0 = 0.07 \pm 0.02$. This is also shown in Fig. 4 where $\omega_{\text{peak}}^{-1}$ and $\tau_0(Wi)$ are shown to scale similarly with Wi . Interestingly, MD simulations (including explicit solvent) and BD simulations of a free draining chain yield the same value of $\omega_{\text{peak}}\tau_0$: 0.08(4) and 0.07(5), respectively. In order

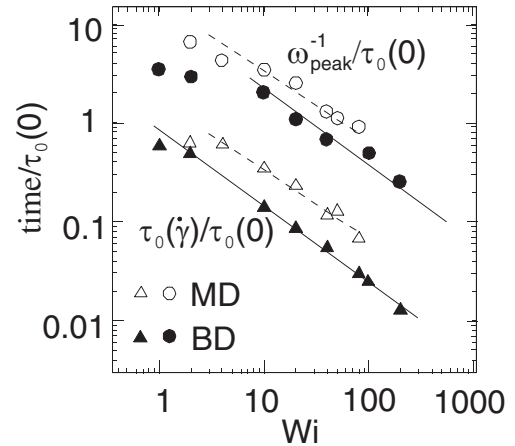


FIG. 4. Reciprocal of the peak frequency $\omega_{\text{peak}}^{-1}$ of the cross power spectral density (circles) and the chain longest relaxation time in flow $\tau_0(Wi)$ (triangles) versus the Weissenberg number. Times are scaled with $\tau_0(0) = 2000\tau$ (MD results) or $\tau_0(0) = 4000\tau$ (BD results). Solid lines (best fits to BD results) are $0.9Wi^{-0.78}$ and $12Wi^{-0.78}$ and dashed lines $1.6Wi^{0.70}$ and $19Wi^{0.70}$.

to check any dependence on the chain length N we performed BD simulations with $N = 30$, obtaining a similar outcome $\omega_{\text{peak}}\tau_0 = 0.06$ (see Fig. 3). These facts indicate that the resonant mechanism illustrated in Fig. 1 is quite general and it fixes a similar ratio between the preferred cycling period and the chain relaxation time, in chains of different length and, with or without explicit solvent representation.

Another quantity of interest is the spread of the CPSD around the peak frequency. As an estimation, we calculated the ratio of the cross power at the peak frequency ω_{peak} and that at $0.2\omega_{\text{peak}}$. This ratio reaches a maximum value around $Wi = 10$ and substantially decreases at the longest Wi considered (see the CPSD for $Wi = 100$ in Fig. 3). Thus, the cycling behavior of the tethered polymers under shear is best observed at $2 < Wi < 20$, while at large enough $Wi > O(100)$ the range of cycling times broadens and the cross spectra does not present such a clear dominant frequency.

To conclude, the analysis of the long-time dynamics of a tethered chain in shear flow demonstrates the existence of a characteristic cycling time, revealed in the cross power spectra of the chain extension in flow and gradient directions. Both the main cycling time $\omega_{\text{peak}}^{-1}$ and the longest chain relaxation time in flow τ_0 scale like the time needed to stretch the chain by convection, $t_s \propto (\dot{\gamma}\langle Y \rangle)^{-1}$. However, the main cycling period is comparatively larger, $\omega_{\text{peak}}^{-1} \simeq 14\tau_0$. The ratio between the main cycling time and the relaxation time is found to be similar in free draining chains, chains in explicit solvent, and chains of different lengths, meaning that these recursive dynamics are quite general.

Long recursive times introduce memory into the fluid, with important consequences in non-Newtonian rheology (for instance, a stronger flow-gradient correlation explains why grafted chains create larger normal stress than free chains in shear flow [10].) Long characteristic times associated with this coil-stretch recursive dynamics favor friction reduction at solid-fluid surfaces: grafted chains, strained by the flow, exert their elastic stress back to the fluid within delay times longer than their relaxation time. Also, as suggested by previous authors [2], the large increase in normal stress at certain resonant frequencies in oscillatory shear flow [4] could be related to the excitation of low frequencies of polymer dynamics. Knowledge on these frequencies offers important clues for the investigation of these puzzling effects.

The author thanks J.J. Freire for useful remarks, S. Barsky for her visualization code, and P.V. Coveney for support. This work was supported by Spanish Grants No. CTQ2004-05706/BQU and No. FIS2004-01934 and the Marie-Curie European Reintegration Grant No. MERG-CT-2004-006316.

*Electronic address: rafa@ccia.uned.es

- [1] D. E. Smith and S. Chu, *Science* **281**, 1335 (1998).
- [2] P. Doyle, B. Ladoux, and J.-L. Viovy, *Phys. Rev. Lett.* **84**, 4769 (2000).
- [3] P. LeDuc, C. Haber, G. Bao, and D. Wirtz, *Nature (London)* **399**, 564 (1999); D. E. Smith, H. P. Babcock, and S. Chu, *Science* **283**, 1724 (1999).
- [4] S. Warburg, J. Klein, and D. Perahia, *Nature (London)* **352**, 143 (1991).
- [5] B. Xue and W. Wang, *J. Chem. Phys.* **122**, 194912 (2005).
- [6] G. Baldini, F. Cannone, and G. Chirico, *Science* **309**, 1096 (2005).
- [7] C. Jeppesen, J. Wong, T. L. Kuhl, J. N. Israelachvili, N. Mullah, S. Zalipsky, and C. M. Marques, *Science* **293**, 465 (2001).
- [8] T. Halioglu, I. Bahar, and B. Erman, *J. Chem. Phys.* **105**, 2919 (1996).
- [9] B. Ladoux and P. Doyle, *Europhys. Lett.* **52**, 511 (2000).
- [10] A. S. Lemak, N. K. Balabaev, Y. N. Krnet, and Y. G. Yanovsky, *J. Chem. Phys.* **108**, 797 (1998).
- [11] The solvent and chain beads interact through a purely repulsive LJ potential, while interactions with wall are LJ with an increased cutoff ($r_c = 1.25\sigma$) and energy scale ($\sqrt{1.7}\epsilon$) ensuring no slip at the wall. We used the velocity Verlet algorithm, with a time step $\delta t = 0.0075\tau$, and a Langevin thermostat for motions in the normal-to-flow directions was used to kept a constant temperature $K_B T = 1.0\epsilon$. The bulk solvent density was $\rho \simeq 0.8\sigma^{-3}$.
- [12] K. Kremer and G. Grest, *J. Chem. Phys.* **92**, 5057 (1990).
- [13] S. Barsky, R. Delgado-Buscalioni, and P. V. Coveney, *J. Chem. Phys.* **121**, 2403 (2004).
- [14] R. Delgado-Buscalioni and P. V. Coveney, *Phys. Rev. E* **67**, 046704 (2003); R. Delgado-Buscalioni, E. Flekkøy, and P. V. Coveney, *Europhys. Lett.* **69**, 959 (2005).
- [15] In MD simulations, due to nonlinear interactions, $\{\hat{\mathbf{R}}_p\}$ are not completely uncorrelated. However, we observe that $\langle \hat{\mathbf{R}}_p \hat{\mathbf{R}}_q \rangle^2 / (\langle \hat{\mathbf{R}}_p^2 \rangle \langle \hat{\mathbf{R}}_q^2 \rangle) \leq 0.05$, for $p \neq q$, thus providing a good approximation to the normal modes.
- [16] Y. Marciano and F. Brochard-Wyart, *Macromolecules* **28**, 985 (1995).
- [17] Scalings proposed for $\langle Y \rangle \sim \dot{\gamma}^\kappa$ are based on the Graetz-Leveque argument (balance between the convective transport $\langle Y \rangle \dot{\gamma}$ and the transverse bead diffusion $D / \langle Y \rangle^2$). However, different scalings for the bead diffusivity $D \sim \langle Y \rangle^\beta$ were used: In Refs. [18–20], $\beta = \{-2/3, -1, 0\}$ respectively, providing $\kappa = \{-3/11, -1/4, -1/3\}$. The balance of flow drag and elastic forces [9] also gives $\kappa = -1/3$.
- [18] J. Hur, E. S. G. Shaqfeh, and R. G. Larson, *J. Rheol. (N.Y.)* **44**, 713 (2000).
- [19] R. Jendrejack, J. de Pablo, and M. Graham, *J. Chem. Phys.* **116**, 7752 (2002).
- [20] P. S. Doyle, E. S. G. Shaqfeh, and A. P. Gast, *J. Fluid Mech.* **334**, 251 (1997).
- [21] G. C. Carter and J. F. Ferrie, in *Programs for Digital Signal Processing*, edited by D. S. P. Committee (IEEE Press, New York, 1979).